

01 **Nonequilibrium Phase Transition**
02 **in Scattered Cell Communities Coupled**
03 **by Auto/Paracrine-Like Signalling**
04
05

06
07 **H. Berry**
08
09
10
11
12

13 **Abstract** Auto/paracrine cell-to-cell communications via diffusive messengers can
14 be coupled to a positive feedback loop in which cell stimulation by a messenger
15 results in the production of new messengers. This yields a potential mechanism
16 for relay transmission of the emitted message. This paper investigates the influ-
17 ence of noise on this mutual coupling of the cells with their environment, using
18 numerical simulations of a stochastic minimal model. The results demonstrate that
19 the deterministic (mean-field) approximation of this stochastic process fails short
20 of predicting its behaviour because of the presence of strong noise-induced fluc-
21 tuations. Instead, the behaviour of the model can be explained by the occurrence
22 of a nonequilibrium phase transition, which is found to be in the universality class
23 of directed percolation. This provides a theoretical framework to understand signal
24 transmission in these stochastic systems.
25

26 **Keywords** Signal transmission · autocrine relay · stochastic models · critical
27 phenomena · directed percolation
28
29

30 **1 Introduction**
31

32 Complex behaviours in cell communities such as self-organization and emergent
33 phenomena may result from coupling of the cells with an environment they dynam-
34 ically modify. For instance, cells often respond to molecules in their environment
35 via intracellular signalling pathways that eventually result in altered concentration
36 of the very extracellular molecular species that triggered the pathway.

37 A well-known example is auto/paracrine signalling. In this paradigm, cells emit
38 a peptidic factor (e.g. EGF) that diffuses in the extracellular space until it reaches a
39 neighbouring cell (paracrine signaling) or the source cell that emitted it (autocrine
40 signaling) (Wiley et al., 2003). Stimulation by the diffusive factor may in turn trigger
41

42
43

H. Berry
44 INRIA, Team Alchemy, Parc Club Orsay Université, 3, rue J. Rostand, 91893 Orsay Cedex France
45 e-mail: hugues.berry@inria.fr

01 intracellular signalling cascades (e.g. the MAPK pathway) that eventually lead to
02 the release of new diffusive factor molecules in the environment (positive feedback
03 loop) (Pribyl et al., 2003a; Freeman, 2000).

04 Strikingly, this process can be considered as a rather generic communication
05 pattern, that is not restricted to members of the EGF family or cytokines, but is
06 also encountered in cAMP-mediated communications between *Dictyostelium dis-*
07 *coideum* cells; acylated homoserine lactone-mediated quorum sensing in *Vibrio*
08 *fischeri* (James et al., 2000) and other bacteria (de Kievit & Iglewski, 2000); or
09 even airborne virus spreading – which has been implied in the dissemination of the
10 foot-and-mouth disease (Gloster et al., 2005) or the influenza virus flu (Hammond
11 et al., 1989) for instance.

12 Although dissimilar, these examples share common features. First, the messenger
13 travels at random, through diffusional or nondirectional transport. Moreover, en-
14 counter with the messenger molecule alters cell functioning in such a way that new
15 messengers are ultimately excreted. Finally, stimulation by the messenger molecules
16 is usually followed by a refractory or lag period during which the cell does not
17 respond to new encounters with messenger molecules.

18 Broadly speaking, this process can be thought of as implementing relay broad-
19 casting: “if a message is received, relay it to one of your nearest neighbours”. Hence,
20 though the spatial range of a single messenger molecule may be limited (Shvartsman
21 et al., 2001), the presence of the feedback loop may allow messages to be transmitted
22 over long distances, very much like the spreading of epidemics. For instance, in a
23 detailed deterministic continuous biophysical model, Pribyl et al. (2003a) showed
24 that this kind of relay autocrine signalling may give rise to messenger travelling
25 waves that spread over the entire cell population.

26 However, like many processes in cell biology, this mechanism comes with inher-
27 ent noise or stochasticity at several levels. First, because of the diffusive nature of
28 the messenger movements, the target cell of an emitted messenger is random, i.e.
29 cannot be precisely specified. Secondly, because it relies on intrinsically stochastic
30 biochemical reactions, the triggering of an intracellular signalling pathway upon
31 cell-messenger molecule interaction is probabilistic. Finally, at every moment, a
32 messenger molecule can be removed from the system, either by extracellular prote-
33 olysis, or by scavenging in the extracellular space.

34 In recent years, several papers have presented biophysical models for auto/
35 paracrine signalling. However, to the best of our knowledge, these studies con-
36 sisted either in deterministic models of auto/paracrine relay transmission (Pribyl
37 et al., 2003a,b) or in stochastic models for messenger-cell interactions, but without
38 feedback relay loops (Batsilas et al., 2003; Shvartsman et al., 2001).

39 The goal of the present work is thus to study the influence of noise in auto/
40 paracrine-like relay broadcasting systems. In particular, it investigates the collective
41 behaviour exhibited by the mutual coupling between cells and their environment,
42 and how messages can be transmitted in stochastic conditions. In this framework,
43 we focused on the basic mechanisms underlying these generic processes, and vol-
44 untarily restricted our model to the elementary ingredients identified above. The re-
45 sults demonstrate that classical deterministic modelling fails to predict the behaviour

01 observed in stochastic simulations because of large fluctuations due to the intrinsic
 02 noise. Moreover, we show that the behaviour of this stochastic system is due to
 03 the occurrence of a nonequilibrium phase transition and present evidence that this
 04 nonequilibrium phase transition is in the universality class of directed percolation.

05

06

07 **2 The Model**

08

09 As already mentioned above, we are interested here in the most fundamental pro-
 10 cesses implied in auto/paracrine-like relay signalling. Hence, we study a “min-
 11 imal” model that incorporates only the few basic ingredients enumerated above
 12 (messenger diffusion, feedback-positive loop for messenger relay, refractory phase).
 13 Furthermore, the model is intrinsically stochastic regarding cell stimulation by mes-
 14 senger molecules, as well as messenger molecule survival in the extracellular space.
 15 For the same reasons, we study a one-dimensional version of the model, i.e. mes-
 16 senger molecules and cells evolve in a one-dimensional lattice of linear size L with
 17 periodic boundaries (i.e. a circle made of L equidistant lattice sites).

18

19

20

21

22 **2.1 Messenger Molecules**

23

24

25

26

27

28

29

30

31 **2.2 Cells**

32

33

34

35

36

37

38

39

40

41

42

43

44

45

Besides messenger molecules, the lattice also contains n immobile point cells that
 are regularly scattered over the lattice. Each cell occupies a single lattice site, so
 that, as $n < L$, the distance between two nearest-neighbour cells is several lattice
 sites. Each cell $i = 1 \dots n$ is associated with a dynamical variable $\phi_i(t)$ that takes
 integer values between 0 and $K - 1$ and represents the state of cell i at simulation
 time step t . Upon stimulation by a messenger molecule, a cell enters a refractory
 phase which lasts $K - 1$ time steps and during which the cell is not responsive
 to messenger molecules (see Fig. 1). The state $\phi_i = 0$ is the quiescent state. The
 transition from $\phi_i = 0$ to $\phi_i = 1$ represents the stimulation step and occurs with
 probability ω (per time step) if a messenger molecule is present on cell i lattice site.
 Transition from the state $\phi_i = j$ to $\phi_i = j + 1$ then occurs with probability 1 (at
 each time step) for $j = 1 \dots K - 1$. After K steps, the cell is back in the quiescent
 state i.e. goes from $\phi_i = K - 1$ to $\phi_i = 0$ with probability 1. Finally, the transition
 from $\phi_i = K_p$ to $\phi_i = K_p + 1$ ($K_p \in 1 \dots K - 1$) is accompanied by the release of a
 new messenger on cell i lattice site.

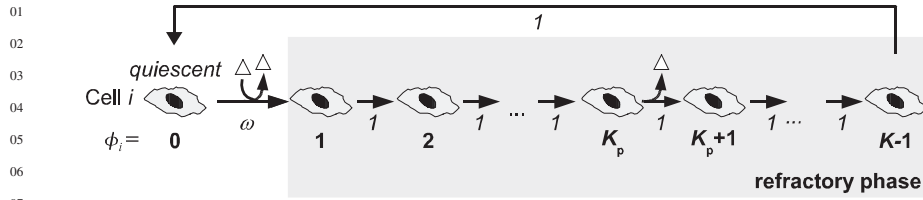


Fig. 1 Overview of the cell activation cycle. In the sequence, the cell state ϕ_i is indicated by a bold number below the cell. Transition probabilities (at each time step) between two cell states are indicated by italicized numbers below corresponding arrows. Intervening messenger molecules are symbolized by white triangles. During the refractory phase of the cycle (*light grey background*), the cell is not sensible to messenger molecules

2.3 Initialization

The initial state of the system corresponds to “full lattice” initial conditions: one messenger molecule is initially positioned *on each* lattice site and the state of each cell $\phi_i(0), \forall i = 1 \dots n$, is randomly chosen from a uniform distribution between 0 and $K - 1$.

2.4 Simulations

Numerical simulations basically implement the above listed rules (Fig. 1, Sections 2.1. and 2.2). For clarity, we present below the translation of these rules in the point of view of the simulation algorithm.

After initialization, the system is updated as follows at each simulation step $t > 0$:

- The state ϕ_i of each cell i is first updated. If a messenger molecule is present on cell i lattice site and if i is quiescent ($\phi_i(t - 1) = 0$), its state is updated to $\phi_i(t) = 1$ with probability ω . Note that, in the presence of m messengers on the same cell site, the effective stimulation probability is $P(\phi_i = 0 \rightarrow \phi_i = 1) = 1 - (1 - \omega)^m$. Cells in the refractory phase ($\phi_i(t - 1) > 0$) are updated according to $\phi_i(t) = \phi_i(t - 1) + 1$ or $\phi_i(t) = 0$ if $\phi_i(t - 1) = K - 1$. Finally, new messengers are created at each cell site for which the updated state variable $\phi_i(t) = K_p + 1$.
- The messenger molecules are then updated according to two substeps. Each messenger is first independently and simultaneously moved to one of its two nearest-neighbour sites (chosen at random). Each molecule is then removed from the lattice with uniform probability λ .

2.5 Parameter Values

Unless otherwise stated, standard parameter values used in the present paper were: $L = 500 \times 10^3$ sites, $n = 50 \times 10^3$ cells, $K = 20$ and $K_p = 10$. For each parameter

01 set, the results presented are averages over 10 different realizations of the initial
 02 conditions and of the simulation run. The system behaviour was mainly studied
 03 through variations of the stimulation probability ω and the messenger removal prob-
 04 ability λ .

05

06

07 **3 General Behaviour**

08

09 **3.1 Mean-Field Analysis**

10

11 To predict the behaviour of the model, a first approach neglects the inherently
 12 stochastic nature of the model and assumes that the fluctuations of the number
 13 of messenger molecules on the lattice are not significant. This so-called “mean-
 14 field” approach fundamentally approximates the model as a *deterministic* process,
 15 using differential equations that are actually similar to the mass-action laws used in
 16 classical (bio)chemical kinetics (see Berry (2003) for further details). Under these
 17 assumptions, the system is predicted to asymptotically reach a steady state (i.e. a
 18 stable fixed point). The messenger density ρ ($= m/L$ where m is the total number
 19 of messenger molecules on the lattice) in the steady state is given by:

20

21

22

23

24

25

26

27

28

29

30

31

32

33

34

35

36

37

38

39

40

41

42

43

44

45

$$\rho^{\text{ss}} = \begin{cases} 0 & \text{if } \omega < \omega_c \\ \frac{1}{K-1} \left(\frac{1}{\omega_c} - \frac{1}{\omega} \right) & \text{if } \omega \geq \omega_c \end{cases} \quad (1)$$

with

$$\omega_c = \frac{\lambda L}{n} \quad (2)$$

Hence, mean-field predictions state that, if $\omega < \omega_c$, messenger molecules are eventually cleared from the lattice (while every cell eventually becomes quiescent). In a way, this corresponds to the death of the system and will be referred to as the “absorbing phase”. Conversely, if $\omega \geq \omega_c$, messenger molecules persist indefinitely on the lattice. This phase will be referred to as the “active phase”.

When ω is close to ω_c , a Taylor series expansion at first order of $(1/\omega_c - 1/\omega)$ is $(\omega - \omega_c)/\omega_c^2$. Thus Eq. (1) can be rewritten as:

$$\rho^{\text{ss}} \propto \omega - \omega_c, \quad \text{for } \omega \rightarrow \omega_c \text{ in the active phase} \quad (3)$$

Figure 2 presents simulation results illustrating the occurrence of the absorbing and active phases. In this figure, the x -axis is the 1-D lattice. A black dot is drawn at each lattice site containing a messenger molecule. The evolution of the system in time is plotted along the y -axis. When ω is small (Fig. 2A), messenger molecules persist for circa 100 time steps, before undergoing massive extinction. Eventually, after ≈ 600 time steps, all the messengers have been removed from the lattice, and

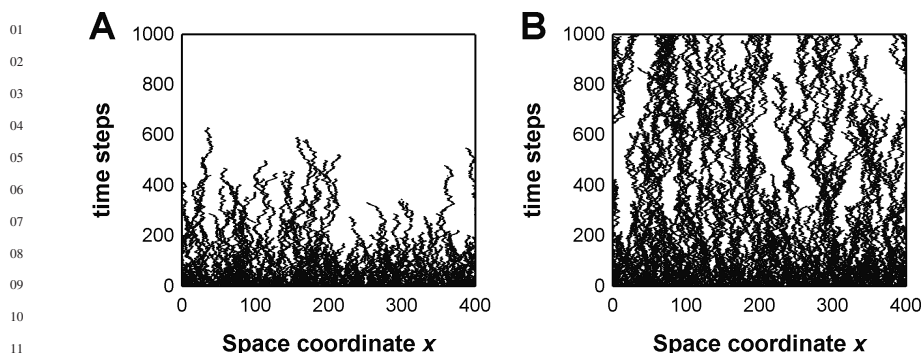


Fig. 2 Simulations of the model illustrating the occurrence of an absorbing (A) and an active (B) phase. Parameters were: $L = 400$ sites, $n = 40$ cells, $K = 20$, $Kp = 10$, $\lambda = 0.0150$ and (A) $\omega = 0.100$ or (B) $\omega = 0.6235$

the system freezes into the absorbing (dead) phase. Conversely, for large ω values (Fig. 2B), the messenger molecules survive for the entire time span of the simulation (active phase). Albeit the system is constantly changing, visual inspection of the figure indicates that messenger density tends to a roughly constant value.

It must however be emphasized that the mean-field analysis above is valid only if the spatial fluctuations of messenger molecules are negligible. Yet simulations of the model such as those presented in Fig. 2 show that at every time step, the distribution of messenger molecules is rather inhomogeneous in space, with “white” zones (devoid of messengers) of various sizes and “black” regions where messenger density is high. This is a fundamental expression of the inherently stochastic nature of the model. It indicates that spatial fluctuations in the system are high, and could invalidate some of the predictions made by the *deterministic* mean-field analysis. To quantify and characterize the behaviour of the system with its natural stochasticity and fluctuations, intensive simulations of the model are needed. The following of the paper is devoted to these analyses.

4 Simulation Results

4.1 Dynamics of the Messenger Density

Figure 3 presents the time evolution for the density of messenger molecules ρ in the active (Fig. 3A) or absorbing (Fig. 3B) phases. In the active phase, ρ decreases according to three main regimes. After an initial slow decay regime (up to ≈ 20 time steps), ρ decreases abruptly for $\approx 10^3$ time steps. Finally, at long times, ρ dynamics reaches a regime where it fluctuates around a constant average value. Fundamentally, this stationary fluctuating regime is the stochastic equivalent of the steady state predicted by the deterministic mean-field analysis (Eq. 1). The average value of the fluctuations at long times in the simulations will thus as well be noted ρ^{ss} .

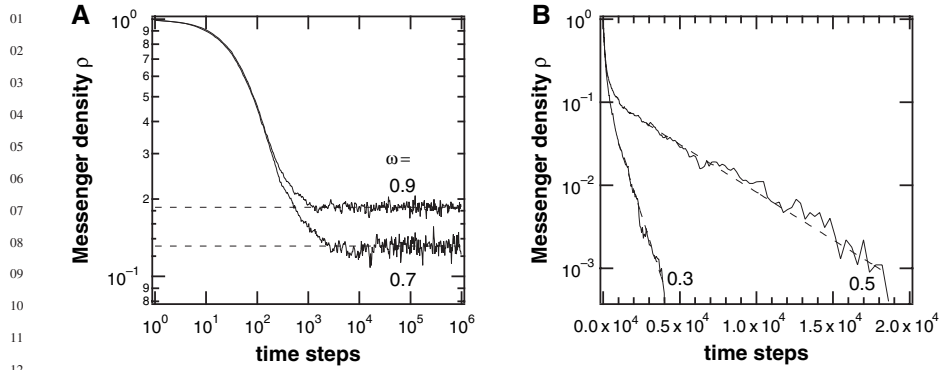


Fig. 3 Dynamics of the messenger density $\rho(t)$. Simulation results for “Full lattice” initial conditions in the active (A) or absorbing (B) phases. In (A) the dashed lines indicate the corresponding average value in the fluctuating stationary state ρ^{ss} . In (B) dashed lines represent fits with exponentially decreasing functions. The values of ω are indicated beside the curves; $\lambda = 0.0150$; $L = 500 \times 10^3$ sites, $n = 50 \times 10^3$ cells, $K = 20$ and $K_p = 10$. Results are from a single simulation run

Note however that, while both simulations and mean-field analysis indicate a stationary state in the active phase at long times, the predicted values are different. For instance, with the parameters of Fig. 3, Eq. (1) predicts $\rho^{ss} = 0.276$ (for $\omega = 0.7$) and 0.292 (for $\omega = 0.9$) while simulations yield 0.131 and 0.186 , respectively. This is a first evidence for failure of the mean-field analysis due to the high fluctuations in the model.

In the absorbing phase (Fig. 3B), the behaviour at long times is quite contrasted. Instead of reaching a stationary regime, messenger density vanishes very fast. Indeed, this curve is plotted in log-linear coordinates so that the observed linear behaviour indicates an exponentially fast decay.

Hence, in the active phase at long times, ρ settles onto a fluctuating stationary regime, while in the absorbing phase, messengers vanish according to an exponential decay. The difference between these two behaviours can be used to identify the boundary between the two phases. Figure 4A shows the dynamics of ρ for values of ω that are close to the transition between active and absorbing phases. For the smallest values of ω (the bottom curves in the figure), the curves bends down. Note that the curves are plotted here in log-log coordinates so that this downward curvature reflects the exponential decay characteristic of the absorbing phase. Conversely, the curves obtained for the largest values of ω (the upper curves in Fig. 4A) inflect upwards and tend towards the stationary state, which is a characteristic of the active phase.

At the boundary between the two phases, i.e. for the critical value ω_c , the decay of ρ at long times is thus expected to be linear in log-log coordinates (neither curving upwards nor downwards), which corresponds to the power-law:

$$\rho(t) \propto t^{-\alpha}, \quad \text{for } \omega = \omega_c, \text{ and } t \rightarrow \infty, \quad (4)$$

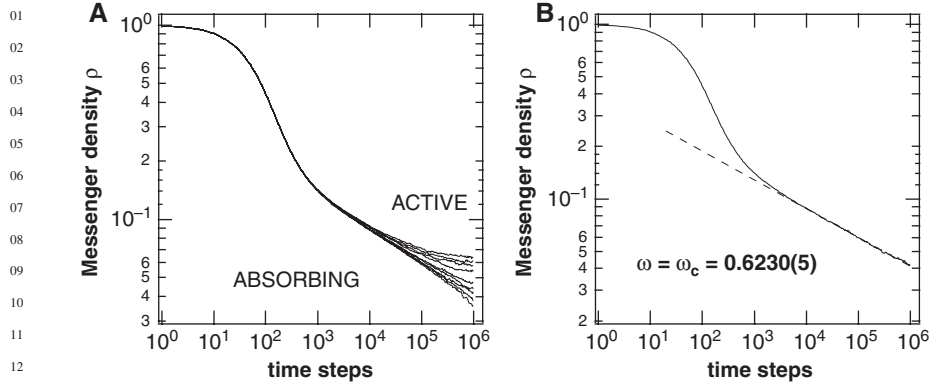


Fig. 4 Dynamics of the messenger density $\rho(t)$ close to the boundary between active and absorbing phases. **(A)** Each curve corresponds to a different value of ω , i.e., from bottom to top, $\omega = 0.6220, 0.6225, 0.6230, 0.6235, 0.6240, 0.6260, 0.6270, 0.6280$ and 0.6290 . **(B)** Time-variation of ρ when ω is set to its estimated critical value $\omega = \omega_c = 0.6230(5)$. (The number between parentheses denotes the estimated incertitude on the last digit). The dashed curve indicates a power-law decay with exponent -0.165 . Parameters were $\lambda = 0.0150$ and other parameters from the standard set (c.f. 2.5)

Hence, the value of ω that yields a power-law behaviour can be used as an estimate for ω_c . Using this principle, Fig. 4B shows that an estimate of $\omega_c = 0.6230$ is obtained. Furthermore the estimated value for the exponent of the corresponding power-law in this case is $\alpha \approx 0.165$. It must be noted that the prediction of the

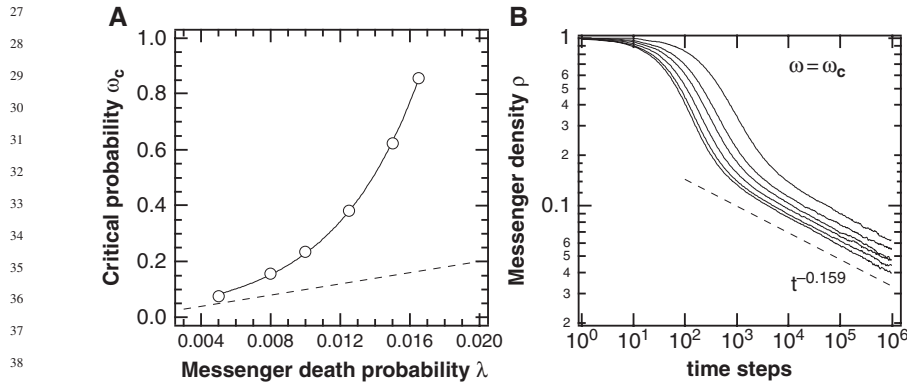


Fig. 5 Critical behaviour for various values of the messenger death probability λ . **(A)** Estimates of the critical stimulation probability ω_c as a function of λ (open circles). The dashed line indicates prediction from the mean-field analysis (Eq. 2). The full line is an exponential fit. **(B)** Dynamics of the messenger density $\rho(t)$ for various values of λ at the corresponding critical value ω_c . λ values are (from top to bottom): 0.0050; 0.0060; 0.0100; 0.0125; 0.0150 and 0.0165. The dashed line indicates a power-law decay with exponent 0.159. All other parameters according to the standard values (Section 5)

01 mean-field analysis fails here. In the case of Fig. 4, (Eq. 2) predicts $\omega_c = 0.150$,
 02 which is less than one fourth of the value obtained in the simulations.

03 The critical behaviour for various values of the messenger death (removal) prob-
 04 ability λ is shown in Fig. 5. Simulations of the model show that the critical value
 05 ω_c increases exponentially fast with λ (Fig. 5A, open circles). Here again, the pre-
 06 diction of the mean-field analysis (Fig. 5A, dashed line) clearly underestimates the
 07 actual value of the critical threshold. The dynamics of ρ for various values of λ at
 08 criticality (i.e. setting ω to its critical value ω_c at the corresponding value of λ) are
 09 plotted Fig. 5B. Albeit the final power-law regimes start at longer times when λ
 10 decreases, all the curves obtained eventually reach a power-law regime with similar
 11 value of the exponent α (i.e. parallel straight lines in log-log coordinates). Averaging
 12 over these simulations, an improved estimate for the exponent α (Eq. 4) is obtained:
 13 $\alpha = 0.159(7)$ (the number between parentheses indicates the estimated uncertainty
 14 on the last digit).

16 4.2 A Nonequilibrium Phase Transition

18
 19 The dependence of the messenger density in the (fluctuating) stationary state ρ^{ss} on
 20 the stimulation probability ω is exemplified in Fig. 6 for $\lambda = 0.0150$. The behaviour
 21 exhibited by ρ^{ss} in the simulations is clearly typical of a (continuous or second-
 22 order) phase transition between the active phase and the absorbing phase. It is for
 23 instance similar to the ferromagnetic phase transition observed in materials such as
 24 iron, where global magnetization increases continuously from zero as the tempera-
 25 ture is lowered below the critical (Curie) temperature¹.

26 However, a fundamental difference between the phase transition observed here
 27 and classical phase transitions lies in its nonequilibrium nature. Indeed, most of the
 28 classical phase transitions (including the ferromagnetic transition) are equilibrium
 29 phenomena, i.e. they obey the so-called “detailed balance” condition (Hinrichsen,
 30 2006): the transition rate (or more precisely fluxes) from any state i to any state j
 31 is equal to that of the reverse transition rate, from j to i . This condition implies the
 32 presence of real equilibrium states and is a fundamental property of these systems.
 33 In particular, it allows applying usual thermodynamic tools and concepts.

34 In the system studied here, the absorbing state induces a violation of the detailed
 35 balance condition: this state can be reached with some probability from the active
 36 state, *but cannot be escaped*. In turn, this prevents the application of several of the
 37 classical thermodynamic concepts. The general properties of these kinds of phase
 38 transitions, called nonequilibrium phase transitions, are thus still a matter of debate
 39

40
 41 ¹ Note that the apparent discontinuity close to the critical value in Fig. 6 is a numerical artefact
 42 due to the so-called “critical slowing down”. Indeed, as the critical threshold is approached, the
 43 fluctuating stationary regime starts at increasingly long simulation times. As this regime has to be
 44 reached to estimate the corresponding value of ρ^{ss} , the number of time steps in the simulations must
 45 be substantially increased as the critical threshold is approached. Hence the apparent discontinuity
 of Fig. 6 only reflects computational limitations hindering measurements with ω values closer to
 the threshold.

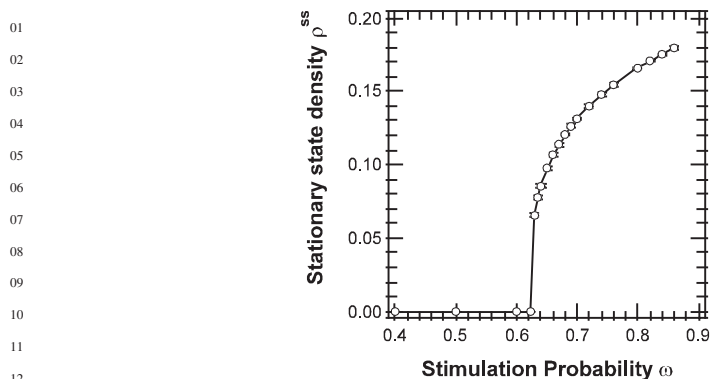


Fig. 6 Variation of the messenger molecule density in the (fluctuating) stationary state, ρ^{ss} , as a function of the stimulation probability ω . Open circles show the results from the simulations of the models (the full line is a guide for the eyes). Parameters were $\lambda = 0.0150$, and standard values for the others. Error bars show ± 1 s.d.

in the physics community, but several points are well established (for reviews see Hinrichsen, 2006, Odor, 2004 or Hinrichsen, 2000a).

Like their equilibrium counterparts, nonequilibrium phase transitions exhibit generic power-law behaviours close to the critical threshold. Equation (4) is a first example of such a power-law, but we will encounter more of them in the following. Several quantities found in the power-laws depend on details of the simulation and the system considered: they are called “non-universal”. For instance, the value of the critical threshold ω_c is known to be non-universal, and thus depends on the probability λ for instance, as seen in Fig. 5A (just like the value of the percolation threshold depends on the type of percolation model considered, i.e. bond or link percolation). However, close to the critical threshold, several quantities (called universal quantities) are largely insensitive to microscopic details of the system (as in equilibrium phase transitions). For instance, the value of the exponent α (the critical exponent of power-law Eq. (4) does not vary when λ changes (Fig. 5B).

One great success of the theory of equilibrium phase transitions is the explanation that transitions arising in different systems can share the same set of critical exponents. This phenomenon is called “universality”. For example, the critical exponents at the liquid-gas critical point are independent of the chemical composition of the liquid. Furthermore, several models for transport in porous media (Sahimi, 1994) share the same critical exponent values as models of sol-gel transitions (Adam & Lairez, 1996): they are in the same universality class (that of percolation, in this case). This means that the dominant processes implied in these systems are explainable by the same fundamental mechanisms.

Nonequilibrium phase transitions may as well be classified into several universality classes. Among them, the universality class of Directed Percolation (DP) has proven the most robust. Apparently very different systems, ranging from population dynamics (Lipowski & Lipowska, 2000), epidemic spreading (Dammer &

01 Hinrichsen, 2003), forest fires (Albano, 1994), biological evolution (Ferreira &
 02 Fontanari, 2002), Ca^{2+} signalling (Timofeeva & Coombes, 2004; Bär et al., 2000)
 03 to morphology dynamics of growing surfaces (Hinrichsen, 2000a), belong to the DP
 04 universality class. This indicates that, beyond their diversity, all these systems rely
 05 fundamentally on the same ground processes. However, several other universality
 06 classes for nonequilibrium phase transitions have been uncovered, such as the par-
 07 ity conserving universality class (Zhong & ben-Avraham, 1995), or the conserved
 08 threshold transfer process universality class (Lübeck & Heger, 2003).

09 Hence, determining the universality class of a nonequilibrium phase transition is
 10 an important step towards the understanding of its fundamental mechanisms. Prac-
 11 tically, this consists in estimating the value of the critical exponents of the system.
 12 This task is carried out in the following sections.

14 4.3 Universality Class of the Phase Transition

15 Besides Eq. (4), an important power-law for nonequilibrium phase transitions relates
 16 the average value of the density of messengers in the fluctuating stationary state, ρ^{ss} ,
 17 to the distance to the critical threshold, $\omega - \omega_c$ (Hinrichsen, 2006):
 18

$$19 \rho^{ss} \propto (\omega - \omega_c)^\beta, \quad \text{for } \omega \rightarrow \omega_c \text{ in the active phase} \quad (5)$$

20
 21
 22 The corresponding critical exponent β is a universal quantity. Actually Eq. (5) is
 23 identical to Eq. (3) with $\beta = 1$, which means that the mean-field analysis predicts
 24 $\beta = 1$. Figure 7 presents simulation results showing how ρ^{ss} varies as a function
 25 of the distance to the threshold for various values of λ . These curves show roughly
 26 parallel straight lines at small distances, indicating a power-law behaviour with a
 27 critical exponent that does not depend on λ . Averaging over the 6 conditions of
 28 the figure, we obtain an estimate of $\beta = 0.29(1)$. Here again, note that the value
 29 predicted by the mean-field analysis is more than threefold the measured one.
 30

31 Another important critical exponent is the exponent related to the temporal cor-
 32 relations (see Section 5), $\nu_{||}$. Theoretical arguments (Hinrichsen, 2006) indicate that
 33 plots of $\rho(t) \times t^\alpha$ as a function of $t \times (\omega - \omega_c)^{\nu_{||}}$ should yield a collapse of the
 34 curves shown Fig. 4A on two curves: every curves corresponding to active phase
 35 conditions should collapse to a single one, while those corresponding to absorbing
 36 phase conditions should collapse to another single one. Hence, finding the value
 37 of $\nu_{||}$ that yields the best collapse of the curves gives an estimate for this critical
 38 exponent.

39 Figure 8 shows the results obtained for $\lambda = 0.0150$ (i.e. Fig. 4A). Using the
 40 estimated value of $\alpha = 0.159$ (see above), the best collapse of the curves (at long
 41 times) was found for $\nu_{||} \approx 1.7$. Similar treatments of the data for other values of λ
 42 yielded comparable quantities (not shown). On average, the estimate for the critical
 43 exponent is $\nu_{||} = 1.66(9)$.

44 A third important critical exponent is the so-called dynamic exponent z . Roughly
 45 speaking, this exponent relates the behaviour of the system to the size of the spatial

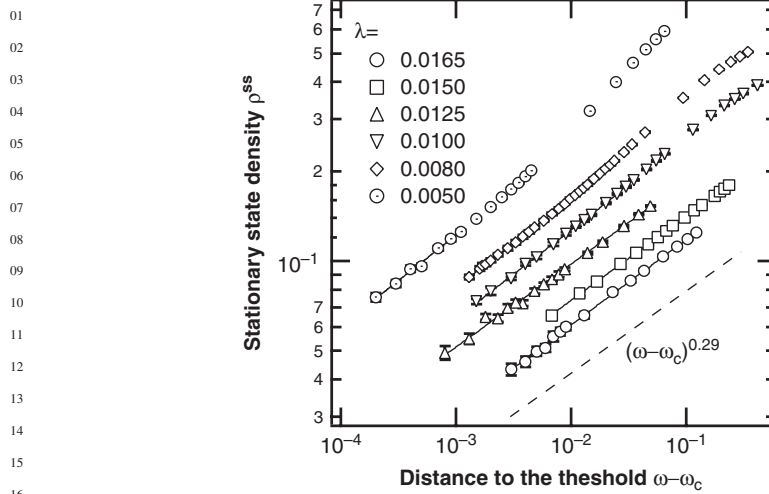


Fig. 7 Scaling of the messenger density in the fluctuating stationary states with the distance to the threshold for different values of the messenger death probability λ . The dashed line indicates a power law with exponent 0.29. All other parameters are set to their standard values. Error bars show ± 1 s.d.

domain (i.e. the number of sites L in the lattice in our case) (Hinrichsen, 2006). It is important to realize that the various power-laws mentioned above are strictly valid for infinite spatial domains only, which is not accessible with computer simulations.

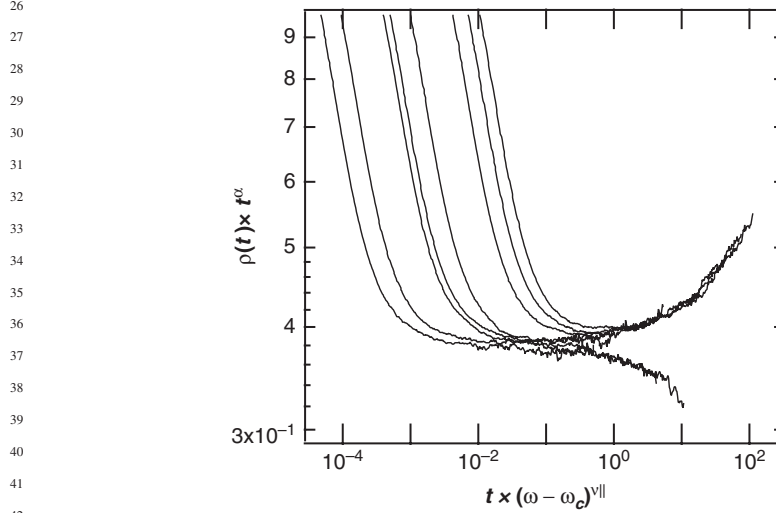
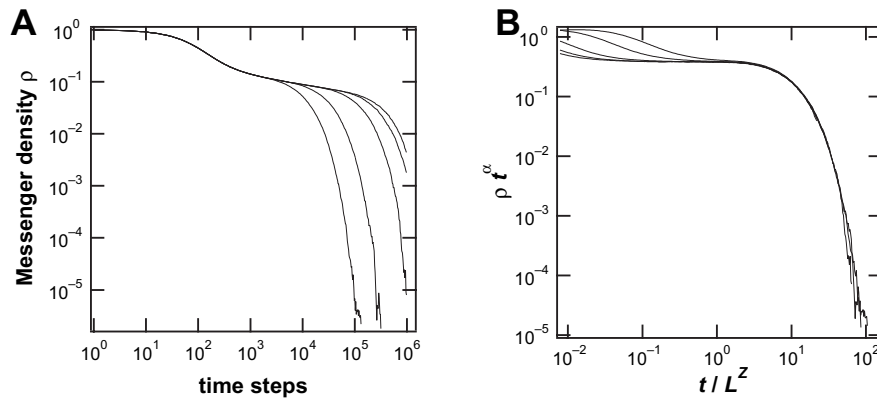


Fig. 8 Scaling test for the value of the critical exponent $\nu_{||}$. The data of Fig. 4A are plotted here as $\rho(t) \times t^\alpha$ as a function of $t \times \omega - (\omega_c)^{\nu_{||}}$ with $\alpha = 0.159$. The best collapse of the curves is obtained for $\nu_{||} = 1.70$. Parameters: $\lambda = 0.0150$ and all other parameters according to their standard values

01 The lattice size used in the simulations presented up to this point ($L = 5 \times 10^5$)
 02 was large enough so that the effects of this finite size could be neglected. In fact,
 03 for simulation durations of 10^6 time steps, we have found that finite size effects are
 04 negligible as soon as $L \geq 5 \times 10^3$ sites.

05 Smaller L values however evidence drastic effects. Figure 9A shows the dynam-
 06 ics of ρ for small lattices ($L \leq 10^3$) at criticality ($\omega = \omega_c$) for $\lambda = 0.0150$ and
 07 constant cell density (i.e. the number of cell is $n = 0.10 \times L$). In this case, the system
 08 has always a certain probability to jump into the absorbing phase (the correspond-
 09 ing curves bend downwards) even though the parameters correspond to the critical
 10 threshold (of course, this probability decreases when lattice size increases, and be-
 11 comes very low for large but finite systems). Theoretical arguments (Hinrichsen,
 12 2006) predict that in this case, plots of $\rho(t) \times t^\alpha$ as a function of t/L^z should yield a
 13 collapse of the curves shown Fig. 9A on a single curve. As with $v_{||}$ above, this gives
 14 a method for estimating the dynamic exponent z . Fig. 9B shows the best collapse,
 15 obtained with $z = 1.55$. The results of Fig. 9 can be replicated using other values
 16 for λ , and yield comparable estimates for z (not shown). The average value obtained
 17 is $z = 1.54(5)$.

18 Table 1 summarizes the values obtained for the four critical exponents estimated
 19 in this study. It also indicates an estimate for the critical exponent related to the
 20 spatial fluctuations, v_\perp . This exponent was not measured directly but deduced from
 21 the definition $z = v_{||}/v_\perp$ (Hinrichsen, 2006). The table also indicates the corre-
 22 sponding values for the directed percolation (DP) universality class in one space
 23 dimension. Clearly, for each exponent, the obtained estimates are in good agree-
 24 ment with those of DP. This demonstrates that the nonequilibrium phase transition
 25 observed in the present model belongs to the directed percolation universality class.



26
27
28
29
30
31
32
33
34
35
36
37
38
39
40
41
42
43
44
45
Fig. 9 Finite size scaling test at criticality ($\omega = \omega_c$) and $\lambda = 0.0150$. (A) dynamics of the mes-
 senger density $\rho(t)$ at criticality for different sizes of the lattice $L = 100; 200; 500; 800;$ and
 1,000 (from *bottom* to *top*). Corresponding values of the number of cells $n = L/10$ (constant cell
 density). (B) Scaling test for the value of the critical exponent z . The data of (A) are replotted here
 as $\rho(t) \times t^\alpha$ as a function of t/L^z with $\alpha = 0.159$. The best collapse of the curves is obtained for
 $z = 1.55$. Parameters: $\lambda = 0.0150$ and all other parameters according to their standard values

Table 1 Comparison of the estimates obtained for the critical exponents studied in the present model and those of Directed Percolation (DP) in one space dimension (values are from Hinrichsen (2006)). Note that the value of z for the present model is not a measure, but is deduced from $z = \nu_{\parallel}/\nu_{\perp}$. Numbers in parentheses indicate uncertainty in the last digit

Model	α	β	ν_{\parallel}	z	ν_{\perp}
Present	0.159(7)	0.29(1)	1.66(9)	1.54(5)	1.08
DP	0.159464(6)	0.276486(8)	1.733847(6)	1.580745(10)	1.096854(4)

5 Message Broadcasting

The characterization of the phase transition allows a better understanding and prediction of several aspects of the model, such as the characteristics of message broadcasting. Let us imagine that the lattice is in the absorbing (dead) phase, i.e. devoid of any messenger molecule, with all cells quiescent. At time t_0 , a single messenger molecule is produced by a cell at a random position on the lattice (see corresponding simulations in Fig. 10). Will this embryo of a message persist over time? Will it finally be transmitted to every cell in the lattice? In physicists' terms, this raises the question of the correlation length in the system. It turns out that, unlike their equilibrium counterparts, nonequilibrium phase transitions possess two independent correlation lengths: a spatial correlation length ξ_{\perp} , and a temporal correlation length ξ_{\parallel} (Hinrichsen, 2000a, 2006). These lengths are directly related to the spreading of the message seed.

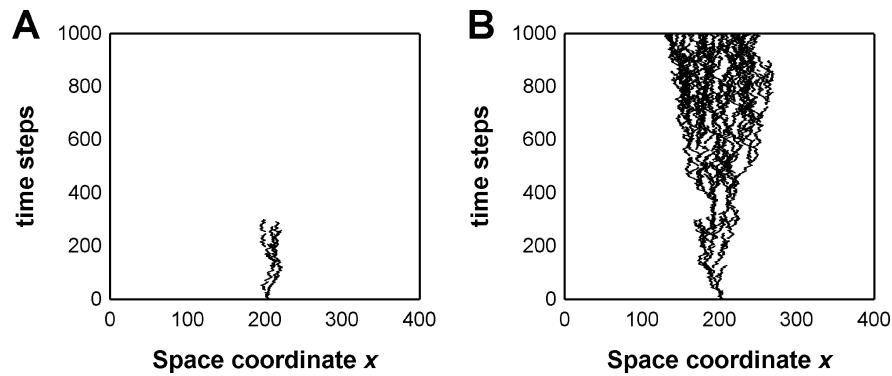


Fig. 10 Simulations of the model illustrating the spreading of a unique initial messenger "seed" in the absorbing phase (A) $\omega = 0.50$ or in the active phase (B) $\omega = 0.95$. Parameters were: $L = 400$ sites, $n = 40$ cells, $K = 20$, $Kp = 10$, $\lambda = 0.0150$. Each cells were initiated in the quiescent state ($\phi_i(0) = 0$; $\forall i = 1 \dots n$)

In the absorbing phase, the message survives for a certain amount of time and tends to slowly expand in space (Fig. 10A). The theory of nonequilibrium phase transition tells us that the average survival time is given by (or at least proportional to) $\xi_{\parallel} \propto |\omega - \omega_c|^{-\nu_{\parallel}}$ and the maximal expansion of the message in space by $\xi_{\perp} \propto |\omega - \omega_c|^{-\nu_{\perp}}$ (Hinrichsen, 2000a). Similarly, in the active phase, message

01 spreads as a cone (Fig. 10B) whose opening angle is given by $\xi_{\perp}/\xi_{\parallel}$. Using these
 02 theoretical concepts, it becomes easy to understand that, as the critical threshold
 03 is approached from below in the simulations, the message spreading from the ini-
 04 tial seed survives for increasing times and reaches a growing fraction of the cells.
 05 At the critical threshold, the effect of a single seed is even eventually transmitted
 06 (relayed) all along the lattice, whatever the physical distance to the initial seed site
 07 (both ξ_{\parallel} and $\xi_{\perp} \rightarrow \infty$). As ω increases further (above the threshold) and enters
 08 the active phase, the opening angle of the spread cone grows as $|\omega - \omega_c|^{\nu_{\parallel} - \nu_{\perp}}$.
 09 Thus, as $\nu_{\parallel} - \nu_{\perp} = 0.637 > 0$ in DP, the time needed for the message to invade the
 10 whole lattice decreases with increasing ω . Hence identifying the phase transition
 11 allows predicting both qualitatively and quantitatively the behaviours shown by the
 12 simulations.

13

14

15 6 Discussion

16

17 The idea that the stochasticity inherent to cellular processes has a strong influence
 18 on elementary behaviours such as toggle switch properties (Tian & Burrage, 2006;
 19 Vilar et al., 2003), clock oscillations (Suel et al., 2006) or signal transduction
 20 (Bhalla, 2004), has recently emerged as a new paradigm in cell biology (for a review,
 21 see Rao et al., 2002). Furthermore, the role played by noise and stochasticity at the
 22 cell or organism level is beginning to be realized (for recent reviews see Samoilov
 23 et al., 2006 or Raser & O'Shea, 2005).

24 The results of the present work add auto/paracrine-like relay signalling to the list
 25 of basic cell processes that may be highly influenced by noise-induced fluctuations.
 26 Our main objective was to study the influence of noise in a model for stochastic com-
 27 munications where cells respond to a diffusive environment that they themselves
 28 have produced through a positive feedback loop. Using numerical simulations, we
 29 showed that the deterministic (mean field) approximation of this process fails short
 30 of predicting the behaviour of the system. Instead, the latter could be understood as
 31 a nonequilibrium phase transition that was evidenced to be in the universality class
 32 of directed percolation.

33 That the model belongs to the directed percolation universality class is actu-
 34 ally not totally unexpected. Indeed, DP has been conjectured (Grassberger, 1982)
 35 to be the universality class of models exhibiting a phase transition from a fluc-
 36 tuating active phase to a unique absorbing phase; whose dynamic rules involve
 37 only short-range processes; and that have no unconventional attributes such as ad-
 38 ditional symmetries (the actual conditions are in fact a bit more restrictive, see
 39 Hinrichsen, 2000a). The present model verifies these conditions thus supporting this
 40 conjecture.

41 Modelling studies of auto/paracrine relay transmission have rarely been ad-
 42 dressed so far. In two studies, Pribyl and coworkers (Pribyl et al., 2003a,b) proposed
 43 a mechanistic model that presents similarities with the model studied here. Their
 44 model takes messenger diffusion, reversible binding to cell surface receptors and a
 45 positive feedback from ligand binding to new ligand release. The main differences

01 with our model are that the feedback mechanism in their model is slightly more
02 detailed (from a biochemical perspective) and most notably, their model is *purely*
03 *deterministic*. Hence, from a stochastic point of view, this model could be consid-
04 ered as a mean-field limit. These authors show that their model supports travelling
05 wave solutions that spread throughout the cell layer. In these waves, the front con-
06 nects a steady state with nonzero messenger density to a steady state devoid of
07 messengers. These behaviours are at first sight reminiscent of the spreading waves
08 encountered in directed percolation, for instance for “seed” initial conditions (see
09 Section 5), and of the active and adsorbing stationary states. Whether this model is
10 related to directed percolation is however not trivial and would necessitate further
11 works. For instance, the spreading waves in DP are not travelling waves (i.e. the
12 shape of the wave front changes during its propagation). Starting from the discrete
13 version of their model (Pribyl et al., 2003b), biologically realistic stochastic pro-
14 cesses could be introduced at several points. Possible phase transitions and univer-
15 sality class of the resulting model could then be assessed through the study of the
16 time evolution of the probability $P(t)$ that a spreading waves survives up to time t ,
17 that scales in the subcritical regime as $P(t) \sim t^{-\delta}$ with $\delta = 0.1595$ or 0.451 for DP
18 in $d = 1$ or 2 dimensions, for instance.

19 Biological interpretation of the present work must be handled with great care.
20 Indeed, the aim of the present work was to study the basic mechanisms at play in
21 such kinds of diffusive communications, so that we voluntarily restricted the model
22 to a set of a few elementary ingredients. Of course, this limits the biological realism
23 of the model, and raises the question of the persistence of the observed behaviours
24 in more detailed and biologically plausible models. While this question can only be
25 answered by further modelling and simulation works, we give here some remarks
26 related to this point.

27 First of all, the universality class of a phase transition is, by definition, not
28 changed by details of the model. And directed percolation, in particular, has proven
29 a very robust universality class to this respect. Hence, it seems unlikely that minor
30 modifications in the model (such as changing the lattice geometry or using off-lattice
31 conditions, using stochastic refractory periods for the cells. . .) would modify dras-
32 tically the observed behaviour. For instance, preliminary investigations showed that
33 changing the values of the cycle parameters (K and K_p) modifies the value of the
34 critical threshold but not the transition itself. Actually, shorter cycle lengths K (not
35 shown) decrease the duration of the initial phase i.e. the non power-law regime of ρ
36 dynamics (the first 10^3 time steps in Fig. 4B).

37 An important parameter is the Euclidean dimension of the lattice. We choose
38 here to study a one-dimensional model because 1-D models are much cheaper
39 in computation time, thus allowing intensive simulations. However, biological re-
40 alism would rather impose two-(or three-)dimensional spaces. Actually a two-
41 dimensional version of the model presented here has previously been studied in
42 Berry, (2003). However, because simulations in this previous paper were not refined
43 enough, the universality class could not be determined unambiguously. Hence, fu-
44 ture work will focus on intensive simulations of the model in two and three space
45 dimensions.

01 Furthermore, another significant assumption in the present work is the regular
02 spacing of the cells on the lattice. However, preliminary simulations (not shown)
03 indicate that random cell positioning does not modify the occurrence of the nonequi-
04 librium phase transition, but has the deleterious effect that the density of messenger
05 molecules decays as a power-law in the absorbing phase (and not exponentially, as
06 observed for regular spacing)². This invalidates the estimation of the critical thresh-
07 old based on the criterion of regime change between subcritical and critical condi-
08 tions, that was used in Fig. 4, for instance. While more computationally expensive,
09 other methods based on finite-size effects for instance (Ortega et al., 1998; Binder
10 & Heermann, 1997) can however be applied in this case and will be used in future
11 studies of the model with random cell positioning.

12 A surprising point concerning directed percolation is that in spite of its amazing
13 robustness in models/simulations, this critical behaviour has still not been evidenced
14 in experiments (see Hinrichsen, 2000b). Hence, the possibility that autocrine relays
15 may provide experimental evidence of DP should be considered seriously. Possi-
16 ble experimental setups could for instance consist in cell and tissue culture assays,
17 where a confluent (or subconfluent) layer of autocrine cells is covered by a liquid
18 medium, in which the soluble messenger is secreted and diffuses. Alternatively,
19 such a situation is naturally found in *Drosophila* eggs (see Pribyl et al., 2003b).
20 The evolution of messenger concentration in the liquid or of related reporters could
21 be monitored in situ, for instance using fluorescence. Such in situ recordings of
22 spatio-temporal evolutions are already accessible to cell biologists (see e.g. Nikolic
23 et al., 2006). Now, messenger death probability (λ in the present model) could
24 be modulated through the addition of various levels of proteinases (degrading the
25 messenger) in the liquid medium. Likewise, the stimulation probability ω could be
26 modulated through the addition of various levels of antagonists of the messenger
27 receptor, or intracellular inhibitors of the signalling pathway supporting the positive
28 feedback. Finally, the A431 carcinoma cell line could be a good candidate for these
29 studies (Dent et al., 1999).

31 References

- 32 Adam M., & Lairez, D., 1996, Sol-gel transition. In *Physical Properties of Polymeric Gels*
33 (J.P. Cohen Addad, ed.), John Wiley & Sons, UK, pp. 87–142.
34 Albano, E.V., 1994, Critical behaviour of a forest fire model with immune trees, *J. Phys. A* **277**:
35 L881–L886.
36 Bär, M., Falcke, M., Levine, H., & Tsimring, L.S., 2000, Discrete stochastic modeling of calcium
37 channel dynamics, *Phys. Rev. Lett.* **84**:5664–5667.
38 Batsilas, L., Berezhkovskii, A.M., & Shvartsman, S.Y., 2003, Stochastic model of autocrine and
39 paracrine signals in cell culture assays, *Biophys. J.* **85**:3659–3665.
40 Berry, H., 2003, Nonequilibrium phase transition in a self-activated biological network, *Phys. Rev.*
41 *E* **67**:031907.

42
43
44 ² Note that this phenomenon has already been encountered in the literature; see Szabo et al. (2002)
45 for instance.

- 01 Bhalla, U.S., 2004, Signaling in small subcellular volumes. I. Stochastic and diffusion effects on
02 individual pathways, *Biophys. J.* **87**:733–744.
- 03 Binder, K., & Heermann, D.W., 1997, *Monte Carlo Simulation in Statistical Physics*, Springer,
04 Berlin, Germany.
- 05 Dammer, S.M., & Hinrichsen, H., 2003, Epidemic spreading with immunization and mutations,
06 *Phys. Rev. E* **68**:016114.
- 07 De Kievit, T.R., & Iglewski, B.H., 2000, Bacterial quorum sensing in pathogenic relationships,
08 *Infect. Immun.* **68**:4839–4849.
- 09 Dent, P., Reardon, D.B., Park, J.S., Bowers, G., Logsdon, C., Valerie, K., Schmidt-Ullrich, R.,
10 1999, Radiation-induced release of transforming growth factor alpha activates the epidermal
11 growth factor receptor and mitogen-activated protein kinase pathway in carcinoma cells, lead-
12 ing to increased proliferation and protection from radiation-induced cell death, *Mol. Biol. Cell*
13 **10**:2493–2506.
- 14 Ferreira, C.P., & Fontanari, J.F., 2002, Nonequilibrium phase transition in a model for the origin
15 of life, *Phys. Rev. E* **65**:021902.
- 16 Freeman, M., 2000, Feedback control of intercellular signalling in development, *Nature*
17 **408**:313–319.
- 18 Gloster, J., Freshwater, A., Sellers, R.F., & Alexandersen, S., 2005, Re-assessing the likelihood of
19 airborne spread of foot-and-mouth disease at the start of the 1967–1968 UK foot-and-mouth
20 disease epidemic, *Epidemiol. Infect.* **133**:767–783.
- 21 Grassberger, P., 1982, On phase transitions in Schlögl’s second model, *Z. Phys. B* **47**:365–374.
- 22 Hammond, G.W., Raddatz, R.L., & Gelskey, D.E., 1989, Impact of atmospheric dispersion and
23 transport of viral aerosols on the epidemiology of influenza, *Rev. Infect. Dis.* **11**:494–497.
- 24 Hinrichsen, H., 2006, Non-equilibrium phase transitions, *Physica A* **369**:1–28.
- 25 Hinrichsen, H., 2000a, Nonequilibrium critical phenomena and phase transitions into absorbing
26 states, *Adv. Phys.* **49**:815–958.
- 27 Hinrichsen, H., 2000b, On possible experimental realizations of directed percolation, *Braz. J. Phys.*
28 **30**:69–82.
- 29 James, S., Nilsson, P., James, G., Kjelleberg, S., & Fagerström, T., 2000, Luminescence control
30 in the marine bacterium *Vibrio fischeri*: An analysis of the dynamics of lux regulation, *J. Mol.*
31 *Biol.* **296**:1127–1137.
- 32 Lipowski, A., & Lipowska, D., 2000, Nonequilibrium phase transition in a lattice prey-predator
33 system, *Physica A* **276**:456–464.
- 34 Lübeck, S., & Heger, P.C., 2003, Universal finite-size scaling behavior and universal dynamical
35 scaling behavior of absorbing phase transitions with a conserved field, *Phys. Rev. E* **68**:056102.
- 36 Nikolic, D., Boettiger, A., Bar-Sagi, D., Carbeck, J., & Shvartsman, S., 2006, Role of boundary
37 conditions in an experimental model of epithelial wound healing, *Am. J. Physiol. Cell Physiol.*
38 **291**:C68–C75.
- 39 Odor, G., 2004, Universality classes in nonequilibrium lattice systems, *Rev. Mod. Phys.*
40 **76**:663–724.
- 41 Ortega, N.R.S., Pinheiro, F.S., Tomé, T., & Drugowich de Felicio, J.R., 1998, Critical behavior of
42 a probabilistic cellular automaton describing a biological system, *Physica A* **255**:189–200.
- 43 Pribyl, M., Muratov, C.B., & Shvartsman, S.Y., 2003a, Long-range signal transmission in autocrine
44 relays, *Biophys. J.* **84**:883–896.
- 45 Pribyl, M., Muratov, C.B., & Shvartsman, S.Y., 2003b, Discrete models of autocrine cell commu-
nication in epithelial layers, *Biophys. J.* **84**:3624–3635.
- Rao, C.V., Wolf, D.M., & Arkin, A.P., 2002, Control, exploitation and tolerance of intracellular
noise, *Nature* **420**:231–237.
- Raser, J.M., & O’Shea, E.K., 2005, Noise in gene expression: origins, consequences, and control,
Science **309**:2010–2013.
- Sahimi, M., 1994, *Applications of Percolation Theory*, Taylor & Francis, UK.
- Samoilov, M.S., Price, G., & Arkin, A.P., 2006, From fluctuations to phenotypes: the physiology
of noise, *Sci. STKE* **366**:re17.

- 01 Shvartsman, S.Y., Wiley, H.S., Deen, W.M., & Lauffenburger, D.A., 2001, Spatial range of au-
02 tocrine signalling: modelling and computational analysis, *Biophys. J.* **81**:1854–1867.
- 03 Suel, G.M., Garcia-Ojalvo J., Liberman, L.M., Elowitz, M.B., Tian, T., & Burrage, K., 2006, An
04 excitable gene regulatory circuit induces transient cellular differentiation, *Nature* **440**:545–550.
- 05 Szabo, G., Gergely, H., & Oborny, B., 2002, Generalized contact process on random environments,
06 *Phys. Rev. E* **65**:066111.
- 07 Tian, T., & Burrage, K., 2006, Stochastic models for regulatory networks of the genetic toggle
08 switch, *Proc. Natl. Acad. Sci. USA* **103**:8372–8377.
- 09 Timofeeva, Y., & Coombes, S., 2004, Directed percolation in a two-dimensional stochastic fire-
10 diffuse-fire model, *Phys. Rev. E* **70**:062901.
- 11 Vilar, J.M., Guet, C.C., & Leibler, S., 2003, Modeling network dynamics: the lac operon, a case
12 study, *J. Cell Biol.* **161**:471–476.
- 13 Wiley, H.S., Shvartsman, S.Y., & Lauffenburger, D., 2003, Computational modeling of the EGF-
14 receptor systems: a paradigm for systems biology, *Trends Cell Biol.* **13**:43–50.
- 15 Zhong, D., & ben-Avraham, D., 1995, University class of two-offspring branching-annihilating
16 random walks, *Phys. Lett. A* **209**:333–337.
- 17
18
19
20
21
22
23
24
25
26
27
28
29
30
31
32
33
34
35
36
37
38
39
40
41
42
43
44
45